Chalcogenide Letters Vol. 17, No. 2, February 2020, p. 49 - 57

INFLUENCE OF Mn ON STRUCTURAL, OPTICAL AND ELECTRICAL PROPERTIES OF $Cu_2(Zn_{1-x}Mn_x)SnS_4$ THIN FILMS DEPOSITED BY SPRAY PYROLYSIS

O. MOHAMMED CHERIF [a,*], A. MEFTAH [a], N. ATTAF [b], A. KABIR [a]
[a]*LRPCSI, Faculty of Sciences, Université 20 août 1955-Skikda, 21000 Skikda, Algeria.*
[b]*Thin Films and Interfaces Laboratory, Frères Mentouri Constantine University, 25000 Constantine, Algeria.*

$Cu_2Zn_{1-x}Mn_xSnS_4$ thin films were deposited onto glass substrates by spray pyrolysis method. They were characterized by X-ray diffraction (XRD), energy dispersive X-ray spectroscopy (EDS) and UV-Visible spectroscopy and the four point probe techniques in order to study the effect of Mn on structural, optical and electrical properties of the samples. Definite x variable like ratio [Mn]/([Zn] + [Mn]) has been taken equal to 0, 0.2, 0.4, 0.6, 0.8 and 1. XRD and EDS analysis revealed the substitution of Mn in Zn sites. $Cu_2MnSn_3S_8$ compound has appeared as a secondary phase in the films deposited with $x \geq 0.6$. Optical band gap of the films increased from 1.34 to 1.68 eV with the increasing x value in the films deposited with ($0.4 \leq x \leq 1$). The resistivity decreases from 1.89 to 0.36×10^{-2} Ω.cm as a result of Sn amount in the film.

(Received October 10, 2019; Accepted February 6, 2020)

Keywords: CZTS, Thin films, Spray pyrolysis, Solar cells

1. Introduction

Solar cells based on Cu(In,Ga)Se_2 and CdTe absorber layers have attained an efficiency of 21.1% [1] and 18% [2], respectively. Nevertheless, there are issues encountered with these absorbing materials, such as the scarcity of In, Ga and Te and the toxicity of Cd. This drawback may limit the mass production of solar cells based on these materials. These problems have stimulated the research for an alternative absorber layer that can be prepared with abundant and environmentally friendly materials. In this context, during the past several years, quaternary semiconductor Cu_2ZnSnS_4 (CZTS) has attracted great attention as one of the most promising absorber layers in solar cells because the zinc and tin elements are more safety, abundant and cheap than indium and gallium constituents of CIGS [3]. Furthermore, CZTS compound has two advantages for efficient solar cells. First, its direct band gap is about 1.5 eV and second its absorption coefficient is over than 10^4 cm^{-1} in the visible light region [4,5]. These fundamental properties promote CZTS to be a good alternative material for photovoltaic conversion. This material can be prepared by a variety of techniques such as electrodeposition [6], co-evaporation [7,8], pulsed laser deposition [9], sputtering [10,11], sol-gel [12,13], spray pyrolysis [14-17], etc...

During the last decade, in order to enhance the quality of CZTS absorber layer, some of other metals were used as substituting or adding to the zinc leading to development of a new semiconductors as Cu_2XSnS_4 (X = Fe, Mn, Co and Ni). These compounds have been also reported as interesting materials for absorber thin films in solar cells due to their structural and optical properties similar to those of CZTS [18,19]. The results reported by the last authors concerning the substitution of Zn by Mn fabricating Cu_2MnSnS_4 (CMTS) absorber material for solar cells show that the material obtained is an excellent candidate for absorber materials owing to its suitable direct band gap with a high absorption coefficient. Also, it is well known that the Mn is more abundant in earth comparing to Zn [3]. Moreover, the cation disorder formed by Cu_{Zn} and Zn_{Cu} anti-site defects can limits the performance in CZTS based solar cells [20], the substitution of Zn^{2+}

*Corresponding author: oussamalmd@hotmail.fr

cation by another cation with larger size can reduce the cations disorder in CZTS [21]. Therefore, in addition to the more abundance of Mn than Zn, the radius of Mn (r_{Mn}^{2+} = 0.80 Å) is relatively high than that of Zn (r_{Zn}^{2+} = 0.74 Å) [22,23] and that can lead to reduce cations disorder in CMTS compared to those in CZTS. This transition between the two semiconductors by replace Zn atoms by Mn has motivated authors to investigate the optical and structural properties of Cu_2MnSnS_4 compound and its efficiency in photovoltaic conversion [19,24,25]. Despite that Cu_2MnSnS_4 compound has promising properties to be a good absorber in thin film solar cells, some experimental studies have been reported about its optical and structural properties. Cui et al. [19] and Prabhakar et al. [24] have reported a band gap value of 1.28 eV for CMTS material synthetized by solvothermal method and 1.6 eV for the same material deposited using spray pyrolysis technique [24]. The band gap of Cu_2MnSnS_4 is still under discussion.

Recently, Chen et al. [26] and Guan et al. [27] have synthesized $Cu_2(Zn_{1-x}Mn_x)SnS_4$ thin films by sol-gel method (x = 0; 0.3; 0.7 and 1) and reported a linear decrease in the optical band gap of the films with increasing Mn content. The variations of the band gap were ranged respectively from 1.51 eV to 1.23 eV and from 1.48 to 1.18 eV. Although, the synthesis of $Cu_2Zn_{0.1}Mn_{0.9}SnS_4$ material has been firstly reported by McCabe et al. [28], but their study has been confined only to the investigation of the magnetic properties. To our knowledge, there are only the two cited reports of $Cu_2(Zn_{1-x}Mn_x)SnS_4$ thin films across the entire composition range ($0 \leq x \leq 1$) , and no one has reported the preparation of $Cu_2(Zn_{1-x}Mn_x)SnS_4$ ($0 \leq x \leq 1$) thin films by spray pyrolysis method. In this work, the preparation of $Cu_2(Zn_{1-x}Mn_x)SnS_4$ ($0 \leq x \leq 1$) thin films by spray pyrolysis using a commercial nebulizer to investigate the effect of x ratio on the structural, optical and electrical properties in $Cu_2(Zn_{1-x}Mn_x)SnS_4$ thin films was reported.

2. Experimental details

Copper(II) chloride dihydrate ($CuCl_2.2H_2O$), zinc acetate dihydrate ($C_4H_6O_4Zn$. $2H_2O$), manganese(II) chloride tetrahydrate ($MnCl_2.4H_2O$), tin chloride dihydrate ($SnCl_2.2H_2O$) and thiouria ($SC(NH_2)_2$) were used as chemical sources of different elements of prepared Cu2($Zn_{1-x}Mn_x$)SnS4 films (Cu, Zn, Mn, Sn and S respectively). In order to deposit Cu_2ZnSnS_4, we have dissolved in 50 ml of distilled water the precursors by stirring: 2×10^{-3} mol of $CuCl_2.2H_2O$, 1×10^{-3} mol of $C_4H_6O_4Zn.2H_2O$, 1×10^{-3}mol of $SnCl_2.2H_2O$ and 12×10^{-3}mol of thiourea ($SC(NH_2)_2$). Particularly, to deposit Cu_2MnSnS_4 sample, the same amount (1×10^{-3}mol) of $C_4H_6O_4Zn.2H_2O$ was replaced by $MnCl_2.4H_2O$. To deposit $Cu_2(Zn_{1-x}Mn_x)SnS_4$ films ($0 < x < 1$), the mole ratios x = Mn/(Zn+Mn) in the solution were adjusted according to the desired x value as x = 0.2, 0.4, 0.6 and 0.8. The excess of thiouria in the solutions was used to compensate the loss of sulfur during spraying and the exo-diffusion during the growth of films at high temperature of substrate [29]. To facilitate the salts dissolving, a few drops of hydrofluoric acid (HF) were added in the solutions. Afterwards, each solution containing precursor elements was sprayed onto glass substrates (SLG) using a commercial nebulizer with a flow rate of 0.5 ml/min. The substrate temperature and the spraying duration were fixed at 350°C and 60 min respectively. Before deposition, glass substrates were well cleaned by acetone then ethanol and finally by distilled water in an ultrasonic bath.

The chemical composition of the films was examined using scanning electron microscope (SEM) equipped with dispersive X-ray analyzer (EDS). The crystal structures of the samples were obtained using Philips X'Pert diffractometer with Cu K_α radiation (λ = 1.5406 Å). Optical transmission and the reflectance in the UV–Visible range (200 – 1100 nm) were recorded by UV-1900 Shimadzu spectrophotometer. The thickness of the films was determined using KLA TENCORD-500 profilometer. The electrical resistivity of the films was measured by four-points method using LOCAS LABS model 2400 instrument.

3. Results and discussion

Typical EDS spectra of $Cu_2(Zn_{1-x}Mn_x)SnS_4$ films is reported in Fig. 1. The compositional ratios of elements determined from EDS analysis are shown in Table 1. As we can see; all films containing Mn have a Cu-poor and Sn-rich composition, except the CZTS film, which has a composition nearly stoichiometric. F. Aslan. et al. [30] have observed that with the increasing of PH values, the copper composition increases and tin composition decreases in dip-coated CZTS films. The same results have been reported by R. Sani et al. [31] in electrodeposited CZTS films. However, the Cu-poor and Sn-rich composition in our films ($0.2 \leq x \leq 1$) can be due to the low value of PH in the spraying solutions which can be caused by the dots of hydrofluoric acid (HF) added in the solution contains precursors as mentioned in the experimental details. It is reported that Cu-poor conditions should optimize CZTS solar cell performance [32], while the Sn-rich composition should be avoided to minimize formation of Sn_{Cu} and Sn_{Zn} anti-sites defects which can lead to limit the efficiency in CZTS solar cell [21]. Therefore, an efficiency higher than 11% in CZTSSe based solar cell have been reached with Cu/(Zn+Sn) <1 and Zn/Sn > 1 [33,34]. All films have a slight S-poor composition and it is maybe referred to the volatility of the sulfur [35]. As shown in Table 1; the value of x = [Mn]/([Mn]+[Zn]) in our deposited $Cu_2(Zn_{1-x}Mn_x)SnS_4$ films is very closed to the precursor values of x in the spraying solution, indicating the substitution of Mn by Zn atoms. Fig. 2 shows the SEM images of CZTS (x = 0) and CMTS (x = 1) films. The films are composed with great numbers of small grains attached to each other. The surface morphology of the CMTS film shows smaller grains with a rough compact surface compared to that of CZTS one. The relatively small grain size appearing in the surface of films can be due to the lack of annealing treatment of the samples at higher temperatures than 350 °C. Many authors have reported an improvement of the crystallinity with the thermal treatment in spray deposited CZTS films [36-38].

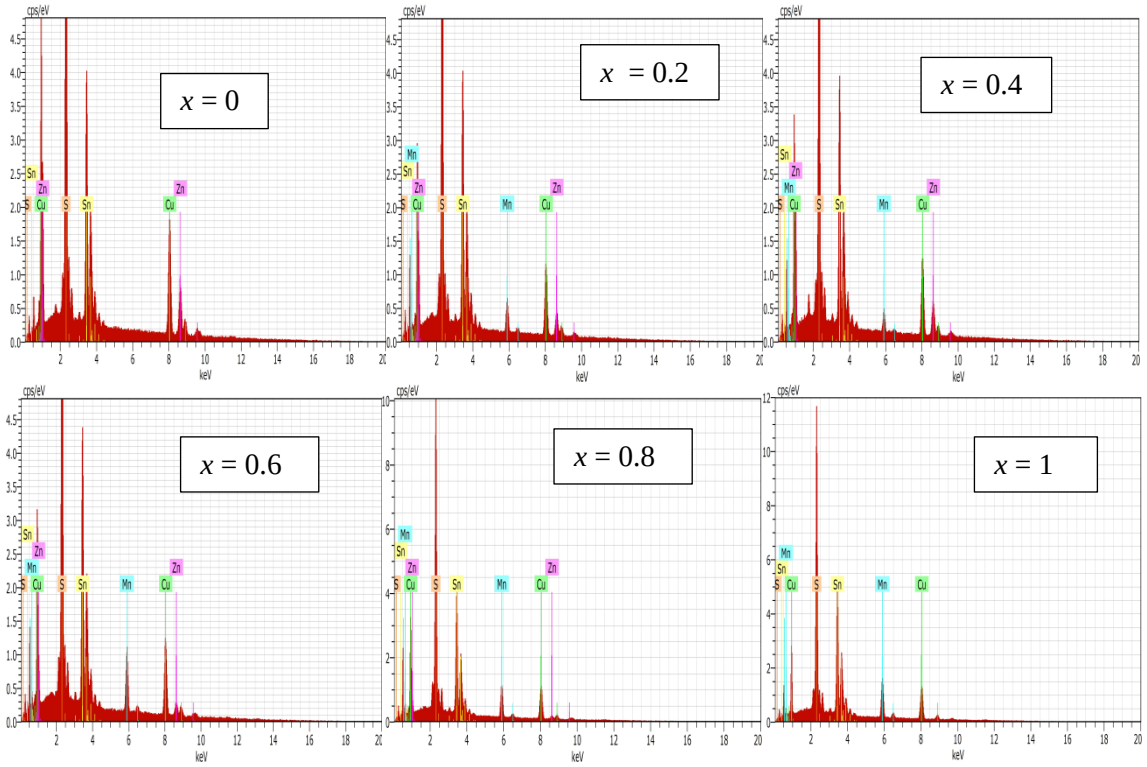

Fig. 1. EDX spectra of $Cu_2(Zn_{1-x}Mn_x)SnS_4$ films.

Table 1. Chemical composition of $Cu_2(Zn_{1-x}Mn_x)SnS_4$ films.

***x*=[Mn]/([Mn]+[Zn]) in precursor**	***x*=[Mn]/([Mn]+[Zn]) in films**	**Chemical composition (at.%)**				
		Cu	Zn	Mn	Sn	S
0.0	0.00	25.44	12.97	0.00	14.33	47.26
0.2	0.23	20.14	10.53	3.14	18.55	47.64
0.4	0.41	19.94	8.04	5.62	19.31	47.09
0.6	0.66	19.82	4.30	8.49	19.88	47.51
0.8	0.83	20.14	2.20	11.35	19.03	47.26
1.0	1.00	20.22	0.00	13.10	19.35	47.33

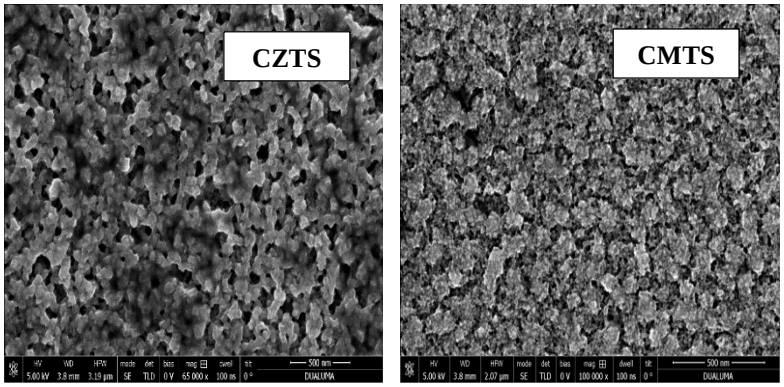

Fig. 2. SEM images of CZTS (x = 0) and CMTS (x = 1) thin films.

The XRD patterns of $Cu_2(Zn_{1-x}Mn_x)SnS_4$ films synthesized with various mole ratios x = 0; 0.2; 0.4; 0.6; 0.8 and 1 are shown in Fig. 3(a). The major diffraction peaks are indexed as corresponding to the (112), (220) and (312) planes of kesterite structure of CZTS (x = 0) and stannite structure of CMTS (x = 1) with (112) as preferential orientation; which are consistent with JCPDS 26-0575 (CZTS) and JCPDS 51-0757 (CMTS) respectively. As observed in the samples synthetized with x = 0.6, 0.8 and 1, four peaks were detected at 2θ = 14.8°, 34.5°, 45.25° and 49.54° which probably attributed respectively to the reflections of (111), (400), (333) and (440) planes of $Cu_2MnSn_3S_8$ phase (JCPDS 51-066). This latter was observed and characterized firstly by Lavela et al. [39]. More recently, Rudisch et al. [40] have deposited Cu_2MnSnS_4 films by reactive co-sputtering method, the formation of $Cu_2MnSn_3S_8$ compound has been observed as secondary phase in all their films deposited with Sn-rich composition, thus the presence of $Cu_2MnSn_3S_8$ as secondary phase in our films is in good agreement with the significant amount of Sn reported in Table 2. The formation of the compound $Cu_2MnSn_3S_8$ is more probable than the formation of $Cu_2ZnSn_3S_8$. It is due in the fact that the formation energy of $Cu_2MnSn_3S_8$ compound from the binary systems ($Cu_2S+MnS+3SnS_2 \rightarrow Cu_2MnSn_3S_8$) is lower than that of $Cu_2ZnSn_3S_8$ from the binary systems ($Cu_2S+ZnS+3SnS_2 \rightarrow Cu_2ZnSn_3S_8$) [40] and that explains why the $Cu_2ZnSn_3S_8$ compound has been not observed in the films with Mn-poor ($x < 0.6$). In addition, in the samples deposited with $x = 0.4$ and 0.8 a weak peak at 26.76° was observed which can be attributed to the reflections of (112) planes of orthorhombic SnS phase (JCPDS 75-2183) [41]. It has been reported that Sn-rich composition in CZTS can lead to the appearance of SnS as secondary phase [42].

Fig. 3(b) shows a large view of (112) peaks. As observed, the peaks are shifted to the lower angles with the increasing of x value, which is attributed to the extension of the lattice parameters due to the relatively larger radius of Mn atoms (r_{Mn}^{2+}= 0.80 Å) than that of Zn atoms (r_{Zn}^{2+}= 0.72 Å) [22, 23]. The lattice constants (a, c) were deduced from XRD data by exploiting the two peaks (220) and (112), using the relation [43]:

$$\frac{1}{d^2} = \frac{h^2+k^2}{a^2} + \frac{l^2}{c^2} \qquad \left(d = \frac{n\lambda}{2sin\theta} \right) \tag{1}$$

As observed in Table 2, with the increasing of x value, the calculated lattice constants (a, c) increase from a = 5.382, c = 10.781 at x = 0 (CZTS) to a = 5.44, c = 10.966 Å at x = 1 (CMTS) and indicates the substitution of Mn atoms in Zn sites. The increase of the lattice parameter in $Cu_2(Zn_{1-x}Mn_x)SnS_4$ films with the increasing of x value has been also observed by Chen et al. [26].

The crystalline size D of the films has been determined from (112) peak using Debye Scherrer's formula [15].

$$D = \frac{0.94\,\lambda}{\beta cos\theta} \tag{2}$$

where λ is the wavelength of the Cu K_α line, β the FWHM of characteristic peak and θ the Bragg's angle. The average crystallite size obtained in all films deposited with various x values are ranged in (7.19 - 7.78 nm).

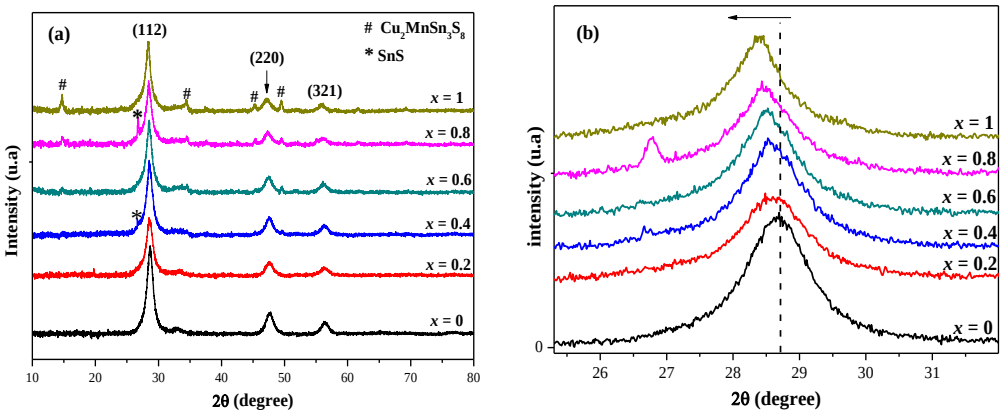

Fig. 3. XRD diffraction patterns of $Cu_2(Zn_{1-x}Mn_x)SnS_4$ thin films(a) and (b) large view of (112) peaks.

Table. 2. Structural characteristics of $Cu_2(Zn_{1-x}Mn_x)SnS_4$ films.

x	Position Pick (112) (2θ°)	FWHM	Particle size (nm)	d_{hkl} (112) (Å)	Lattice constants (a,c) (Å)
0.0	28.68	1.19	7.19	3.109	a=5.382 c=10.781
0.2	28.59	1.19	7.19	3.118	a=5.390 c=10.843
0.4	28.51	1.14	7.51	3.129	a=5.403 c=10.906
0.6	28.48	1.10	7.78	3.131	a=5.413 c=10.887
0.8	28.41	1.10	7.78	3.139	a=5.427 c=10.913
1.0	28.32	1.10	7.78	3.149	a=5.440 c=10.966

In Fig. 4, the optical transmittance and the reflectance spectra in the range (200 - 1100 nm) of the films deposited with different x values are reported. All films have a transmittance lower than 10% in the visible range (400 - 800 nm). In addition, the films have a reflectance lower than 2% in the visible range. These two optical properties indicate the high absorbance of our $Cu_2(Zn_{1-x}Mn_x)SnS_4$ films in the visible range where it is close to 90%. The optical band gaps of $Cu_2(Zn_{1-x}Mn_x)SnS_4$ films were estimated according to Tauc plot [44] by extrapolating the linear part of $(\alpha h\upsilon)^2$ plot and determining the intercept with the hυ axis (Fig. 5). α (cm^{-1}) is the absorption coefficient and hυ (eV) the photon energy. The estimated band gaps Eg of all films (Table 3) are in the range (1.34 - 1.68 eV). As reported in this table, in the films deposited with ($x \leq 0.4$) the band gap estimated to 1.34 eV has been not changed with the increasing of x values. Then, for the ratios ($x \geq 0.6$) the band gap has been increased gradually with the values 1.41; 1.49 and 1.68 eV corresponding to the x values as 0.6; 0.8 and 1 respectively. All these values of the band gaps are appropriate for photovoltaic applications. We can conclude that the substitution of Zn by Mn can control the band gap of $Cu_2(Zn_{1-x}Mn_x)SnS_4$ absorber films. The estimated energy band gap of the CZTS ($x = 0$) is in agreement with that reported by A. Sagna et al. [45], otherwise it is less than the most values reported in the literature (1.45-1.5 eV). They have synthetized CZTS thin films using Close-Space Vapor Transport (CSVT) and have reported a band gap of 1.34 eV for the sample obtained with (Cu/Zn+Sn) = 0.88, which is close to the ratio (Cu/Zn+Sn = 0.93) in our CZTS film as reported in Table 3. According to Sagna et al. [45], this relatively narrow band gap is probably attributed to the presence of high concentration of defects in the thin film such as $Cu_{Zn} + Zn_{Cu}$ and $2Cu_{Zn} + Sn_{Zn}$ defects. Moreover, the optical band gap estimated of CMTS ($x = 1$) is higher than those reported in the references [19, 26, 27]. Chen et al. [26] and Guan et al. [27] have reported that the optical band gap of $Cu_2(Zn_{1-x}Mn_x)SnS_4$ films increases with the increasing of Mn content. However, the enlargement in the band gap in this study with the increasing of Mn content might be caused by the formation of $Cu_2MnSn_3S_8$ as secondary phase. It's clear that the band gap has begun to increase at $x = 0.6$ which coincided with the appearance of $Cu_2MnSn_3S_8$ phase. At our knowledge, there is no experimental band gap of $Cu_2MnSn_3S_8$ compound was reported in the literature.

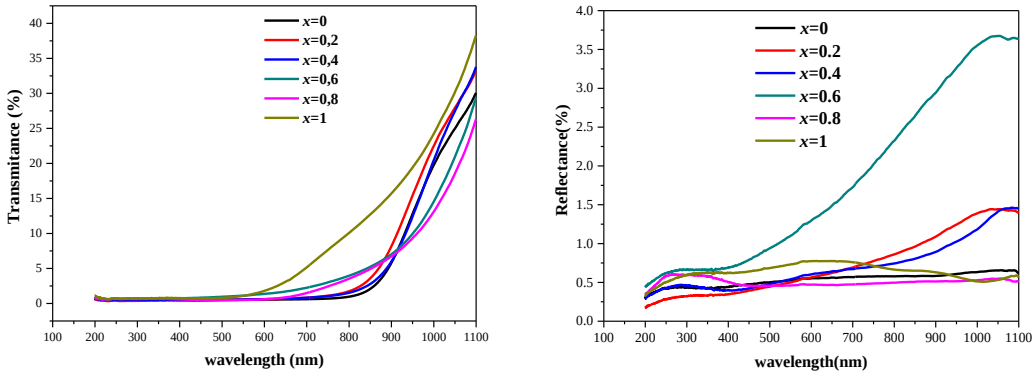

a) *b)*

Fig. 4. Optical spectra of $Cu_2(Zn_{1-x}Mn_x)SnS_4$ films at x various values
(a): Transmittance spectra; (b): Reflectance spectra.

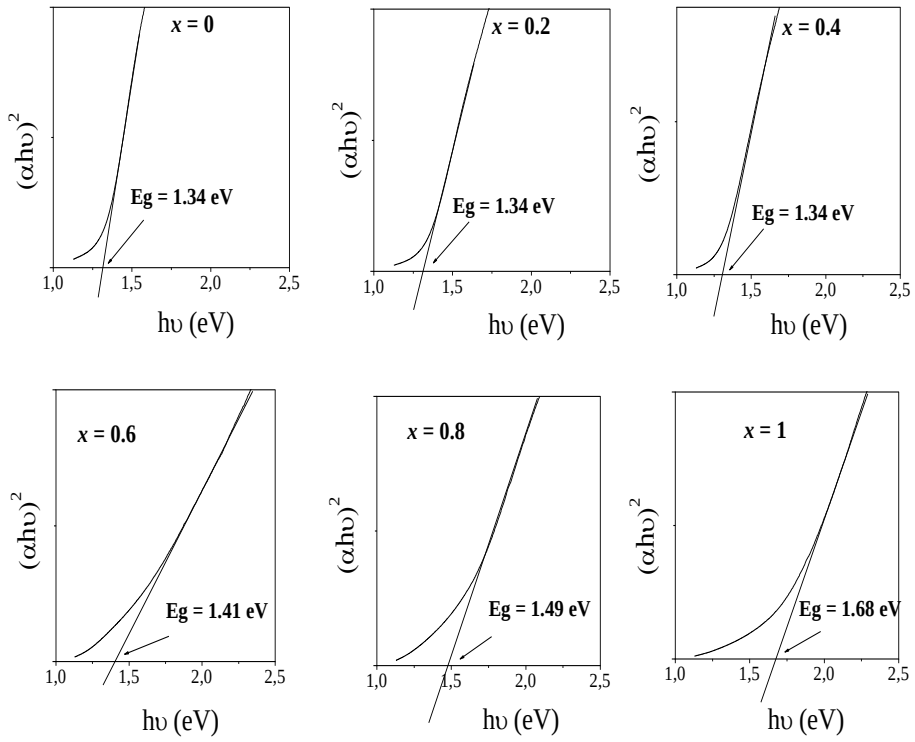

Fig. 5. Plot of variation of the $(\alpha h\upsilon)^2$ as a function of photon energy hυ used for optical gap estimation.

The electrical resistivity of the $Cu_2(Zn_{1-x}Mn_x)SnS_4$ films was measured using four-points method at room temperature. The measured resistivity of the films deposited with various x values accompanied with the corresponding Cu/(Zn+Mn+Sn) and (Zn+Mn)/Sn ratios are reported on Table 3. As it is shown in this Table, a sharp decrease by two order in the resistivity of the films from 1.89 Ω.cm at (x = 0) to 7.27×10^{-2} Ω.cm at (x = 0.2). This significant decreasing in the resistivity has been coincided with a sharp decreasing in (Zn+Mn)/Sn ratio ratios from 0.90 at (x = 0) to 0.74 at (x = 0.2), corresponding to a sharp decreasing in Cu/(Zn+Mn+Sn) ratio from 0.93 at to 0.62. Then, in the range (x > 0.2) the resistivity of the films is ranged in (0.364×10^{-2}-2.87×10^{-2} Ω.cm) and it has been slightly dependent of (x) value. Therefore, the resistivity is predominantly influenced by the amounts of copper and tin in these films and has been not affected by the x value (namely the substitution of Zn atoms by Mn atoms). The relatively low resistivity in the samples deposited with ($x \geq 0.2$) comparing with CZTS (x = 0) sample can be due to their relatively high Sn-rich composition ~ 18 %. Comparatively, Tanaka et al. [46] have studied the influence of the composition elements ratios on the electrical resistivity in CZTS films, the resistivity in their films prepared with Sn-rich composition was relatively lower than those prepared with Cu and Sn-poor. The obtained values of the resistivity in CZTS (x = 0) and CMTS (x = 1) films are in agreement with previous works in the literature [45,47].

Table 3. Electrical resistivity of $Cu_2(Zn_{1-x}Mn_x)SnS4$ films.

x	Cu/(Zn+Mn+Sn)	(Zn+Mn)/Sn	Thickness (μm)	Optical band gap (eV)	Resistivity ($\times10^{-2}$ Ω.cm)
0.0	0.93	0.90	1.06	1.34	189.3
0.2	0.62	0.74	1.15	1.34	1.271
0.4	0.60	0.71	0.89	1.34	0.873
0.6	0.60	0.64	1.22	1.41	2.87
0.8	0.62	0.71	0.97	1.49	1.472
1.0	0.61	0.65	1.02	1.68	0.364

3. Conclusion

$Cu_2(Zn_{1-x}Mn_x)SnS_4$ thin films were deposited on glass substrates by a spray pyrolysis technique using a commercial nebulizer. The effect of x ratio (i.e: Mn content) on structural, optical and electrical properties of $Cu_2(Zn_{1-x}Mn_x)SnS_4$ films has been investigated. XRD analysis showed that kesterite structure of CZTS and stannite structure of CMTS were formed.

The combination of XRD and EDS analysis reveal the substitution of Mn in Zn sites. $Cu_2MnSn_3S_8$ compound appears as a secondary phase in the films deposited with ($0.6 \leq x \leq 1$), the optical band gap of the films increases from 1.34 eV to 1.68 eV with the increasing of x from 0.4 value. The film deposited with x = 0 (CZTS) has a resistivity of 1.893 Ω.cm, while the films deposited with ($0.2 \leq x \leq 1$) have a resistivity ranged in (0.364×10^{-2}- 2.87×10^{-2} Ω.cm).

Acknowledgments

The authors wish their thanks to Professor S. Alleg of Annaba University for the permission to use their XRD facilities.

References

[1] J. Chantana, T. Kato, H. Sugimoto, T. Minemoto, Prog Photovolt Res Appl. **27**(7), 630 (2019).
[2] A. H. Munshi, J. M. Kephart, A. Abbas, T. M. Shimpi, K. L. Barth, J. M. Walls, W. S. Sampath, Sol. Energy Mater. Sol Cells **176**, 9 (2018).
[3] T. Unold, H.W. Schock, Annu. Rev. Mater. Res. **41**, 297 (2011).
[4] K. Ito, T. Nakazawa, Jpn. J. Appl. Phys. **27**, 2094 (1988).
[5] H. Katagiri, K. Saitoh, T. Washio, H. Shinohara, T. Kurumadani, S. Miyajima, Sol. Energy Mater. Sol Cells **65**, 141 (2001).
[6] J. J. Scragg, P. J. Dale, L.M. Peter, Electrochemistry Communications **10**, 639 (2008).
[7] K. Oishi, G. Saito, K. Ebina, M. Nagahashi, K. Jimbo, W. S. Maw, H. Katagiri, M.Yamazaki, H. Araki, A. Takeuchi, Thin Solid Films **517**, 1449 (2008).
[8] T. Tanaka, A. Yoshida, D. Saiki, K. Saito, Q. Guo, M. Nishio, T.Yamaguchi, Thin Solid Films **518**, 29 (2010).
[9] A. V. Moholkar, S. S. Shinde, A. R. Babar, K. Sim, Y. Kwon, K. Y. Rajpure, P. S. Patil, C. H. Bhosale, J. H. Kim, Solar Energy **85**, 1354 (2011).
[10] J. S. Seol, S. Y. Lee, J. C. Lee, H. D. Nam, K. Ho. Kim, Sol. Energy Mater. Sol Cells **75**, 155 003).
[11] J. He, L. Sun, K. Zhang, W. Wang, J. Jiang, Y. Chen, P. Yanga, J. Chu, Applied Surface Science **264**, 133 (2013).
[12] K. Tanaka , Y. Fukui, N. Moritake, H. Uchiki, Sol. Energy Mater. Sol Cells **95**, 838 (2011).
[13] P. K. Sarswat, M. L. Free, Phys. Status Solidi A **208**(12), 2861 (2011).
[14] N. Kamoun, H. Bouzouita, B. Rezig, Thin Solid Films **515**, 5949 (2007).
[15] W. Daranfed, M. S. Aida, N. Attaf, J. Bougdira, H. Rinnert, J. Alloy Compd. **542**, 22 (2012).
[16] O. V. Galán, M. Courel, M. E. Rodriguez, D. J. Olarte, M. A. Frutis, E. Saucedo, Sol. Energy Mater. Sol Cells **132**, 557 (2015).
[17] F. Z. Boutebakh, D. Batibay, M. S Aida, Y. S. Ocak, N. Attaf, Mater. Res. Express **5**(1), 015511 (2018).
[18] D. B. Mitzi, O. Gunawan, T. K. Todorov, K. Wang, S. Guha, Sol. Energy Mater. Sol Cells **95**, 1421 (2011).
[19] Y. Cui, R. Deng, G. Wang, D. Pan, J. Mater. Chem **22**, 23136 (2012).
[20] K. Rudisch, Y. Ren, C. P. Björkman, J. Scragg, Applied physics letters **108**, 231902 (2016).
[21] D. Shin, B. Saparov, D. B. Mitzi, Adv. Energy Mater **7**(11), 1602366 (2017).
[22] V. P. Sachanyuk, I. D. Olekseyuk, O. V. Parasyuk, Phys. Stat. Sol. (a) **203**, 459 (2006).
[23] D. H. Kuo, W. Wubet, J. Alloys Compd. **614**, 75 (2014).

[24] R. R. Prabhakar, S. Zhenghua, Z. Xin, T. Baikie, L. S. Woei, S. Shukla, S. K. Batabyal, O. Gunawan, L. H. Wong, Sol. Energy Mater. Sol Cells **157**, 867 (2016).
[25] S. Marchionna, A. Le Donne, M. Merlini, S. Binetti, M. Acciarri, F. Cernuschi, J. Alloy. Compd. **693**, 95 (2017).
[26] L. Chen, H. Deng, J. Cui, J. Tao, W. Zhou, H. Cao, L. Sun , P. Yang, J. Chu, J. Alloy Compd. **627**, 388 (2015).
[27] H. Guan, H. Shen, J. Li, Chalcogenide Letters **16**, 157 (2019).
[28] G. H. McCabe, T. Fries, M. T. Liu, Y. Shapira, Phys. Rev. B **56**, 6673 (1997).
[29] M. Messaoudi, M. S. Aida, N. Attaf, T. Bezzi, J. Bougdira, G. Medjahdi, Materials Science in Semiconductor Processing **17**, 38 (2014).
[30] F. Aslan, A. Gökta, A. Tumbul, Materials Science in Semiconductor Processing **43**, 139 (2016).
[31] R. Sani, R. Manivannan, S. N. Victoria, J. Electrochem. Sci. Technol. **9**(4), 308 (2018).
[32] S. Chen, X. G. Gong, A. Walsh, S. H. Wei, Applied Physics Letters **96**, 021902 (2010).
[33] W. Wang, M. T. Winkler, O. Gunawan, T. Gokmen, T. K. Todorov, Y. Zhu, D. B. Mitzi, Adv. Energy Mater. **4**(7), 1301465 (2013).
[34] S. G. Haass, M. Diethelm, M. Werner, B. Bissig, Y. E. Romanyuk, A. N. Tiwari, Adv. Energy Mater. **5**(18), 1500712 (2015).
[35] K. Tanaka, N. Moritake, H. Uchiki, Sol. Energy Mater. Sol Cells **91**, 1199 (2007).
[36] M. Valdes, G. Santoro, M. Vazquez, J. Alloys Compd. **585**, 776 (2014).
[37] Z. Seboui, A. Gassoumi, Y. Cuminal, N. Kamoun, Superlattices and Microstructures **75**, 586 014).
[38] L. Dermenji, N. Curmei, M. Guc, G. Gurieva, M. Rusu, V. Fedorov, L. Bruc, D. Sherban, S. Schorr, A. Simashkevich, E. Arushanov, Surface Engineering and Applied Electrochemistry **52**(6), 509(2016).
[39] P. Lavela, J. L. Tirado, J. Morales, J. O. Fourcadeb, J.C. Jumas, J. Muter. Chem **6**(1), 41 1996).
[40] K. Rudisch, W. F. Espinosa-García, J. M. Osorio-Guillén, C. M. Araujo, C. P. Björkman, J. J. S. Scragg, Phys. Status Solidi B **256**(7), 1800743 (2019).
[41] M. Messaoudi, M. S. Aida, N. Attaf, S. Satta, Chalcogenide Letters **16**, 157 (2019).
[42] A. Nagoya, R. Asahi, Physical Review B **81**, 113202 (2010).
[43] A. S. Ibraheam, Y. Al-Douri, U. Hashim, M. R. Ghezzar, A. Addou,Waleed, K. Ahmed, Solar Energy **114**, 39 (2015).
[44] J. Tauc, R. Grigorovici, A. Vancu, Phys. Stat. Sol. **15**, 627 (1966).
[45] A. Sagna, K. Djessas, C. Sene, M. Belaqziz, H. Chehouani, O. Briot, M. Moret, Superlattices and Microstructures **85**, 918 (2015).
[46] T. Tanaka, A. Yoshida , D. Saiki, K. Saito, Q. Guo, M. Nishio, T. Yamaguchi, Thin Solid Films **518**, 29 (2010).
[47] L. Nie, J. Yang, D.Yang, S. Liu, Journal of Materials Science: Materials in Electronics **30**(4), 3760 (2019).